

# Simulating Optimum Egress Time

Kardi Teknomo and Proceso Fernandez

[teknomo@gmail.com](mailto:teknomo@gmail.com) and [pfernandez@ateneo.edu](mailto:pfernandez@ateneo.edu)

Ateneo de Manila University

## Abstract

A standard evacuation map posted in a room shows the location of the current room and the path to the nearest exit. If the number of occupants in the building is only small, then the shortest paths to the exits may enable all the occupants to evacuate in minimum possible time. Previous studies have shown, however, that the shortest path configuration does not lead to minimum egress time for large crowds in public facilities such as those in a school, theater or gym.

We extend the previous studies by determining the minimum egress time for different crowd sizes on a fixed network graph. We apply optimization search on a mesoscopic multi-agent pedestrian simulation that employs the concept of Route Choice Self Organization (RCSO). We show that the egress time gap between the shortest path configuration and RCSO configuration increases very quickly with respect to crowd size. Thus, for crowded pedestrian facilities, there may be a need to revise the standard evacuation map so that evacuation behavior that approximates the RCSO becomes possible, and this can lead to a much better egress time.

**Keywords:** minimum egress simulation, route choice self-organization, shortest path

## 1. Introduction

There are many standards required by government for pedestrian facilities. These standards are enforced to safeguard the lives of the people inside such facilities. One important  
- - - - - 9 - - - - -  
everyone [Tubbs and Meacham, 2007].

To lower the egress time, evacuation maps are normally posted in rooms and other selected areas. Each of these maps shows the location of the current area and the path to the nearest exit. The purpose of these maps is to make people aware of where they should go in case of evacuation so that when the evacuation is needed, they would not spend unnecessary time searching for a way out.

The premise of using the shortest path is that the shorter the distance to be traveled, the less time is needed to cover that distance. However, this fails to consider the fundamental density-flow relationship, which establishes that if more people are on the same path (such as the case when everyone uses the shortest path) then the increased density actually results to decreased speed, and consequently higher egress time.

Therefore, if the number of occupants in a building is only small, then the shortest paths to the exits may enable all the occupants to evacuate in minimum possible time. However, as shown in previous studies [e.g., Teknomo 2008, Schneider and Könecke 2010], the shortest path configuration does not lead to minimum egress time for large crowds. This is not difficult to imagine, since the decrease in speed brought by congestion offsets the advantage of short distance towards the egress point. In any case, the evacuation of large crowds in a public facility such as a school, theater or gym requires special consideration.

We extend the previous studies by determining the minimum egress time for different crowd sizes. We apply optimization search on a mesoscopic multi-agent pedestrian simulation on a fixed network graph that employs the concept of Route Choice Self Organization (RCSO). We show that the egress time gap between the shortest path configuration and RCSO configuration increases very quickly with respect to crowd size. Thus, for crowded pedestrian facilities, there may be a need to revise the standard evacuation map so that an evacuation behavior that approximates the RCSO becomes possible. Doing this may consequently lead to a much better egress time.

This paper is organized as follows. Sections 2 and 3 cover preliminary discussions about the mesoscopic multi-agent pedestrian simulation and the Route Choice Self-Organization, including related literature about these. Section 4 discusses the methodology used in the study. This is followed by a presentation and analysis of the derived results in Section 5. Finally, Section 6 summarizes the main contributions of this paper and proposes some improvements that can lower egress times.

## **2. Mesoscopic Multi-Agent Simulation**

Pedestrian movement can be modeled in the microscopic, macroscopic and mesoscopic levels. A microscopic pedestrian simulation treats each pedestrian as an individual agent that moves about a virtual environment. Each agent is capable of independent action, including pursuit of specific goals and interaction with other agents. This model involves computation-intensive processes and is able to produce very detailed information about the pedestrian flow in some virtual environment. The studies of [Blue and Adler 2000, Helbing and Molnár 1995, Hoogendoorn and Bovy 2004, Kretz and Schreckenberg 2006, Schadschneider 2001, to name a few of them] use this type of model.

On the other extreme, macroscopic pedestrian simulations model the environment using simpler details, and aggregate the pedestrian into groups that follow the fundamental flow-density relations. These models perform fewer computations than microscopic simulation models and are able to produce aggregate information only about the pedestrian system being modeled. Such modeling is the approach used for example by [Henderson 1974, Kachroo and Ozbay 1999 and Lovas 1994].

Our study uses a model strategy that is between the 2 extremes described earlier. Called mesoscopic pedestrian simulation, our model involves aggregating environment information into a network graph, while still treating each pedestrian as an individual agent

in the system. The result is a model with fewer computations than in microscopic models, but with more detailed results than in macroscopic models. Mesoscopic models have been used for studying pedestrian behavior in several papers also [Teknomo and Millionig 2007, Teknomo, Bauer and Matyus 2008]. Slightly more aggregated and different mesoscopic models are also used in other studies [Tolujew and Alcalá 2004, Florian et al, 2001].

In our mesoscopic model, a pedestrian environment is represented by a graph  $G = (V, E)$  where  $V$  is the set of nodes, each representing a critical area of the environment (e.g. door, start or end point of a stair, elevator, escalator, ramp etc.) and  $E$  is the set of edges, each representing direct paths from one node to another. Figure 1 illustrates a sample room layout with the corresponding network graph structure.

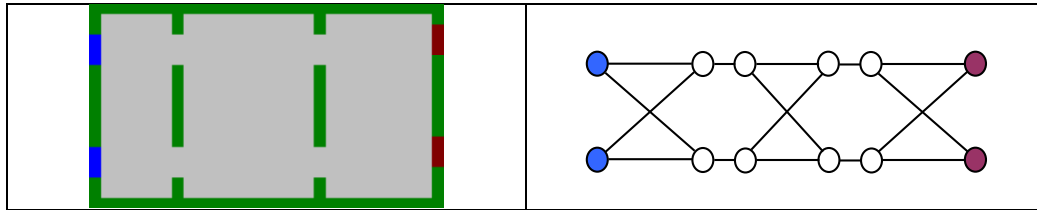


**Figure 1.** A sample floor layout, and the corresponding network graph.

A *source node* in the network graph represents an area where the pedestrians are coming from. The two blue nodes on the left of the network graph in Fig. 1 are source nodes. A *sink node* (e.g., the brown colored nodes on the right most in Fig. 1) corresponds to a target egress point such as an exit door.

Each edge in the graph is assigned an equivalent length and an equivalent width, effectively limiting the maximum number of pedestrians that can simultaneously occupy the space represented by the edge. In this paper this limit is called the *space capacity* of the given edge. For a given edge with length  $l$ , width  $w$  and maximum density  $\rho_{max}$ , the space capacity  $c$  is given by the following equation

$$c = l \cdot w \cdot \rho_{max} \quad (1)$$

A node, on the other hand, is not associated with a capacity value. Since a door is such a crucial element of pedestrian evacuation, which should have an associated capacity, it is modeled by an edge connecting 2 nodes that represent the opposite sides of a door (See Fig. 1). Other crucial elements of the environment, such as stairs, are represented similarly.

In our pedestrian simulation, an agent moves from a source node to a sink node through a valid path in the network graph. The actual path that is selected by an agent, among possibly many path options, is based on the rules described in the next section. By using a network graph instead of a virtual environment, some details are aggregated. This results to a simplified model where there are fewer computations to make.

### 3. Route Choice Self-Organization

The mesoscopic pedestrian simulation that we employ in our study uses a multi-agent system that involves agents moving within a network graph. The path that the agent follows during the simulation is called the *origin-destination path*, or simply OD path.

Traditional multi-agent simulations assign OD paths using either all-or-nothing [Dafermos & Sparrow 1969] or multi-path [Dial 1971] assignment. For a given origin and destination, the all-or-nothing scheme computes the best possible path, i.e., one that minimizes some utility cost function. Then, every agent that starts and ends on the same origin-destination

$$I_{e,t} = 1 - \text{BetaCDF}\left(\frac{\sigma_{e,t}}{c_e}; \theta_1, \phi_1\right) \quad (2)$$

where  $\sigma$  and  $c$  are the pedestrian volume and space capacity, respectively, of the given edge, while  $\theta_1$  and  $\phi_1$  are parameters to the Beta Cumulative Distribution Function. The Beta function has been selected because the graph of its cumulative distribution is flexible enough to handle different varieties of expected volume interaction relationship. For example, when  $\theta_1 = \phi_1 = 1$ , then the graph of the function is simply linear.

**Navigation:** The range of values for this also comes from the interval  $[0, 1]$ . If the attraction component measures the attractiveness of an edge, the navigation component measures the attractiveness of a node at the other end of the edge.

First, every node  $v$  is assigned a value indicating a measure of some utility distance. We have called such assignment as *Sink Propagation Value* (SPV) since the values normally emanate from the sink nodes. Correspondingly, the assignment function is  $SPV(v)$ . One possible assignment function is the measure of actual distance of a node from a nearest sink. In this case,  $SPV(v) = 0$  if  $v$  is a sink node, or  $SPV(v) > 0$  otherwise. Figure 2 illustrates a simple SPV computation for a given network where the edge weights have been pre-assigned.

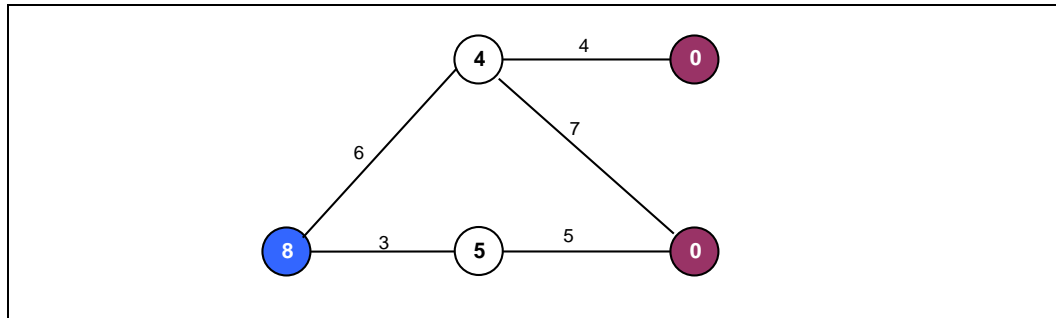


**Figure 2.** SPV computation may be based on shortest distance from a node to a nearest sink.

The navigation value  $N_{i,j}$  from node  $v_i$  to an adjacent node  $v_j$  is a normalized value that also uses the Beta function, as described below.

$$N_{i,j} = \begin{cases} 0 & \text{if } SPV(v_i) \leq SPV(v_j) \\ \text{BetaCDF}\left(\frac{SPV(v_i) - SPV(v_j)}{\max_{v_k \in \Gamma(v_i)} \{SPV(v_i) - SPV(v_k)\}}; \theta_2, \phi_2\right) & \text{otherwise} \end{cases} \quad (3)$$

Here,  $\Gamma(v_i)$  is the set of nodes adjacent to  $v_i$  and having lower SPV than  $v_i$ , i.e., nearer to some sink. The parameters  $\theta_2$  and  $\phi_2$  are used for the Beta distribution function. Note that for static environment such as those where the doors do not open

and close during the simulation, the navigation values need only to be computed at the start of the simulation. This is because the computed SPV for each node is not changed during any part of the simulation.

The movement of the agents in the network graph is modeled using discrete time steps by specifying behavioral update rules at given events. The main types of events are as follows:

1. **Agent insertion:** An agent is inserted into the simulation at a specific time and at a specific source node. For this study, all agents are inserted at the (same) source node at the start of the simulation.
2. **Movement from node to edge:** When an agent is on a node, it must decide which incident edge to take. Let  $v_i$  be the current node of the agent at time  $t$  and let  $v_j$  be an adjacent node from  $\Gamma(v_i)$ . The specific edge  $e = (v_i, v_j)$  that is selected is the one that maximizes

$$k_e = \arg \max_{j \in \Gamma(v_i)} P_{e,t} \cdot I_{e,t} \cdot N_{i,j} \quad (4)$$

Note that although the permission value  $P_{e,t}$  and the navigation value  $N_{i,j}$  are static, the interaction value  $I_{e,t}$  is dynamic, and is dependent on the current situation in the network.

3. **Movement within edge:** Once an agent enters an edge, its speed is computed based on the number of agents ahead and on the same edge, using the fundamental density-flow relationship.

$$speed = speed_{\max} \cdot \left( 1 - \text{BetaCDF} \left( \frac{\sigma_{e,t}}{c_e}; \theta_3, \phi_3 \right) \right) \quad (5)$$

where  $speed_{\max}$  is fixed at 1.2 m/s for all pedestrians.

The agent is assumed to move at this computed speed throughout its stay in the edge. Since the length of the edge is known, then the time that the agent exits the edge and arrives at the next node can be easily determined. The parameters  $\theta_3$  and  $\phi_3$  are used to adjust the cumulative Beta distribution function to control the speed-density relationship. The speed-density follows the Greenshield (1934) linear model when  $\theta_3 = \phi_3 = 1$ . Knowing the speed-density function, the computation of the density-flow relationship is a straightforward application of the fundamental traffic flow formula.

4. **Termination:** An agent is removed from the system once it reaches a sink node. As such, its corresponding pedestrian is considered evacuated from the facility.

The algorithm for the RCSO model that we use in this study is summarized in Fig. 3. The main output is an *NTXY* table, which indicates the *XY* position (in this case, which specific node or edge) of an agent with id *N* at a given time *T*.

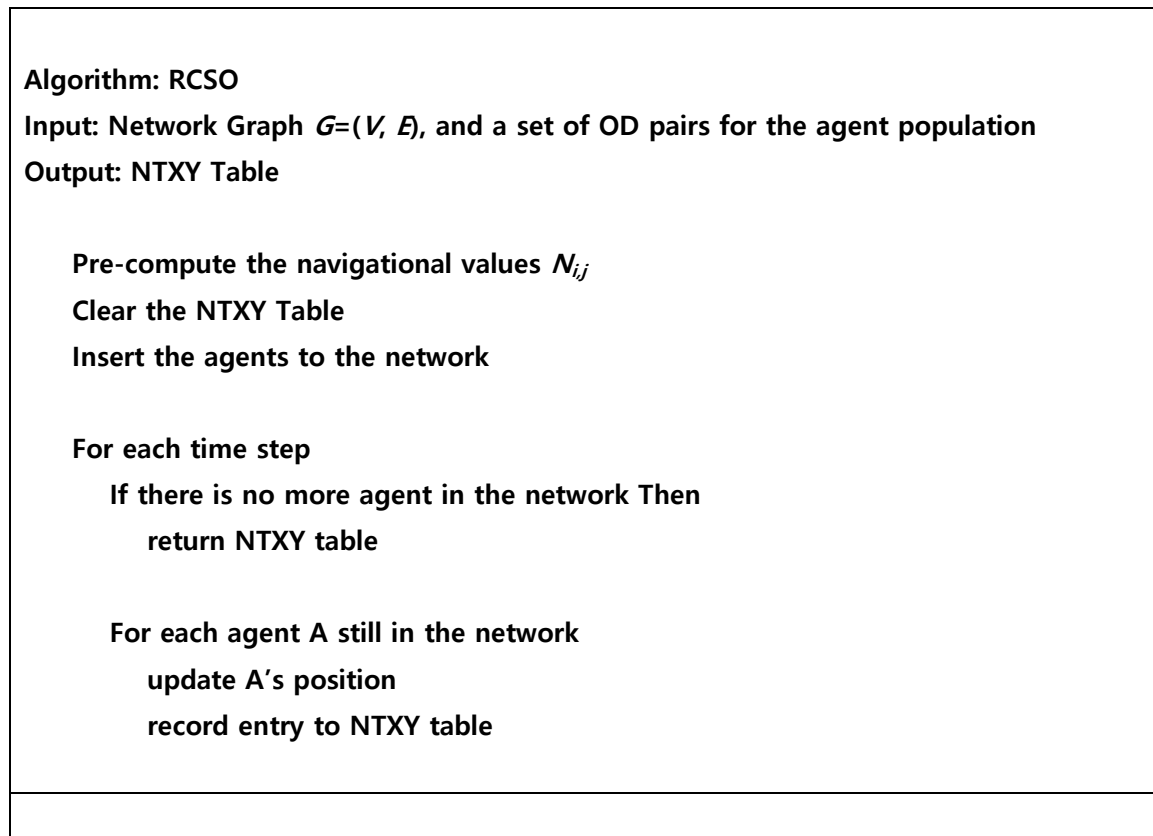


**Figure 3.** Overview of the RCSO algorithm.

#### 4. Methodology

The RCSO model produces a load-balancing effect on a given network. As such, it can be viewed as approximating the minimum possible egress time for a facility. To give us a better understanding of the dynamics of the (approximate) minimum egress time, the numerical experiments for this study were divided into 2 parts, as shown in the figure 4 below

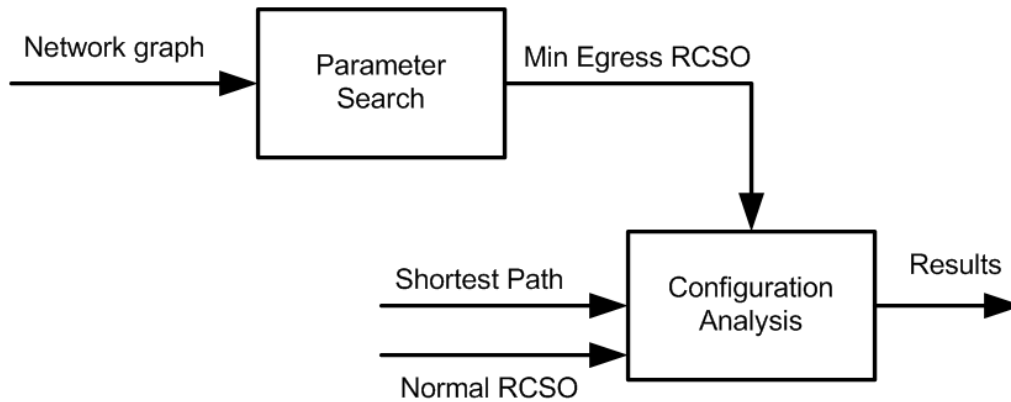


**Figure 4.** Design experiment.

The first set of experiments simulates the minimum egress time using RCSO. However, since the performance of the RCSO depends on the parameter values, we estimate the values that give the minimum egress time using Simultaneous Perturbation Stochastic Approximation (SPSA by Spall, 1998) integrated with Tabu list (Glover, 1989). The set of parameter values that produces the minimum egress time defined what we call the *Minimum Egress RCSO*, in order to differentiate it from *normal RCSO*, which uses the parameter values  $\theta_1 = \phi_1 = \theta_2 = \phi_2 = \theta_3 = \phi_3 = 1$ . The last two parameter values yield a linear relationship for the fundamental diagrams of traffic flow (in term of relationship between space mean speed and density).

The SPSA executed the simulation several times and terminated only when there was no improvement in the results after 500 iterations. For a fixed (relatively simple) network graph and an OD pair set, one simulation may require several seconds to several minutes of run-time. Thus an SPSA optimization search for the same input could run from a few hours to many days.

To derive results within reasonable time, we have decided to use a very simple and yet interesting network graph in this study. The graph contains only 2 nodes (one source and the other sink) connected using 2 edges so as to give pedestrians the chance to select a path (see Fig. 5).

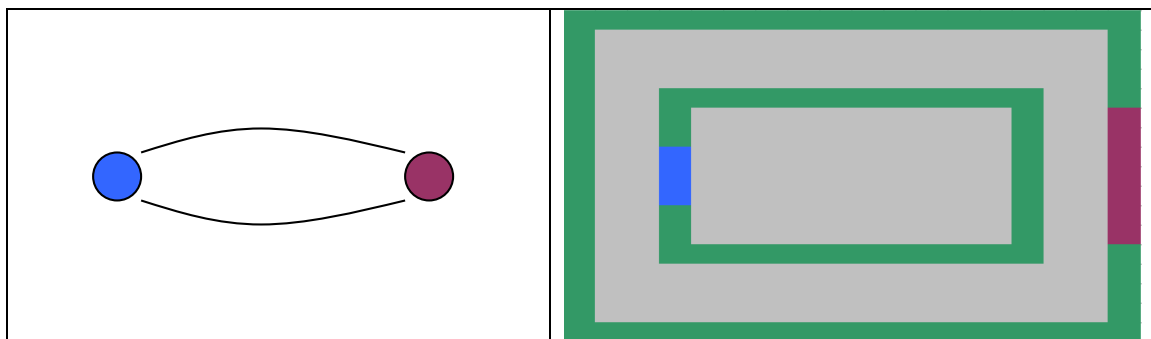


**Figure 5.** Basic network graph used in the experiments, and a possible corresponding floor layout.

After setting up the network graph structure, the lengths and widths of each of the edges, and also the total number of agents in the system were varied in order to determine the relationships among these. The many combinations of variable values also enabled better analysis of the 3 configurations being compared.

The aim in the first set of experiments is to elucidate the relationship of the independent variables to the egress time. To help in this cause, the NTXY table (produced by the simulation with minimum egress time, as returned by the SPSA optimization search) was used to generate the path-usage statistics. The various graphs for the experiments are shown in the section on results.

For the second set of experiments, the results of the previous set of experiments were used to compare with the results of simulations involving normal RCSO and the shortest path configuration. The aim of this part of the study is to validate the hypothesis that as the number of pedestrians in a facility increases, the gap between the egress time of the shortest path configuration and the RCSO configuration increases at a very fast rate.

## 5. Results and Analysis

As mentioned in the previous section, the study is divided into 2 parts. The first part searches for the set of values (for the 6 parameters of the RCSO model) that minimizes the egress time. The second part then compares the egress time of the following configuration models:

1. Minimum Egress RCSO
2. Normal RCSO
3. Minimum Distance Configuration

### 5.1 The Minimum Egress RCSO

After determining the minimum egress RCSO by running the RCSO algorithm on the network graph and then searching for the parameter values that minimize the egress time, the path usage statistic was also collected for each of the various combinations of values for the length, width and number of agents. In particular, these statistics were collected by first fixing the values of  $L_1$  and  $L_2$  (the lengths of the 2 edges) as well as the widths  $W_1$  and  $W_2$  in order to define the exact space capacities ( $C_1 = L_1 W_1$  and  $C_2 = L_2 W_2$ ) of the edges, and then observing how the *ratio* of the path usage between the 2 edges varies with increasing number of agents. Graphing the results on these path usage ratios reveals 4 different patterns emerging. These 4 general patterns are shown in Fig. 6.

In these graphs, the  $x$ -axis is for the number of agents while the  $y$ -axis captures the ratio of the path usage. The blue and red plots correspond to the path usage ratios of the 2 edges. Since there are only 2 edges in the network, the plots exhibit symmetry with respect to the line  $y = 0.5$  (the mean ratio).

### *Pattern 1: One line*

The first pattern revealed involves a straight line. Interestingly, this pattern emerges if and only if the dimensions of the 2 edges are exactly equal (i.e.,  $L_1 = L_2$  and  $W_1 = W_2$ ). Technically, the pattern is not really a straight line, especially on the left part of the plot where there seems to be a large variation. This is actually due to the sensitivity brought about by the small number of agents. For example, if there are only 3 agents, then the best assignment would be one edge having 2/3 path usage ratio while the other having only 1/3.

In general, if the number  $n$  of agents is even, then each of the edges will have exactly  $n/2$  agents passing through it, to yield a usage ratio of 0.5 for both edges. However, if  $n$  is odd, then there will be exactly  $(n+1)/2$  and  $(n-1)/2$  agents passing through the first and second edges respectively. These yield ratios of  $(n+1)/(2n)$  and  $(n-1)/(2n)$  which approximate 0.5 when  $n$  is sufficiently large. Thus, the plot of the path usage ratio approximates that of a line on the mean ratio.

The first pattern strongly demonstrates the load-balancing phenomenon observed in RCSO models. Whenever the 2 edges have equal lengths and equal widths, then even if the number of agents increases, the ratio is still (approximately) 0.5 for each of the edges. Note that the actual optimal configuration for this type of network graph has the same ratio values!

### *Pattern 2: One line with interlinked branches*

Here is where it becomes more interesting. There were plots where the 2 edges have the same ratios of 0.5, until the number of agents reaches a certain threshold. After the threshold, the path usage ratio for one edge starts to increase, while that for the other edge starts to decrease with increasing agent numbers. Two questions come to mind:

- (1) What is the explanation for this behavior in the plot?
- (2) Can the threshold value be predicted?

Each of the 2 edges during this period can still accommodate more agents, and thus receive agents at approximately the same rate. At the threshold point, the two edges are filled up completely, and then afterwards one edge starts to release agents at the other end already.

The 2 edges are filled up (almost) simultaneously even though they have different lengths and widths because their space capacities (length x width) are the same. This concept also helps answer the second question. To determine the threshold point, we only need to compute the maximum total number of agents occupying the 2 edges. Since the length and width values in the experiments are in linear units, then multiplying this with the maximum density for a space will provide the threshold value. The actual formula for the threshold is therefore given by equation

$$threshold = (L_1 \cdot W_1 + L_2 \cdot W_2) \rho_{max} \quad (6)$$

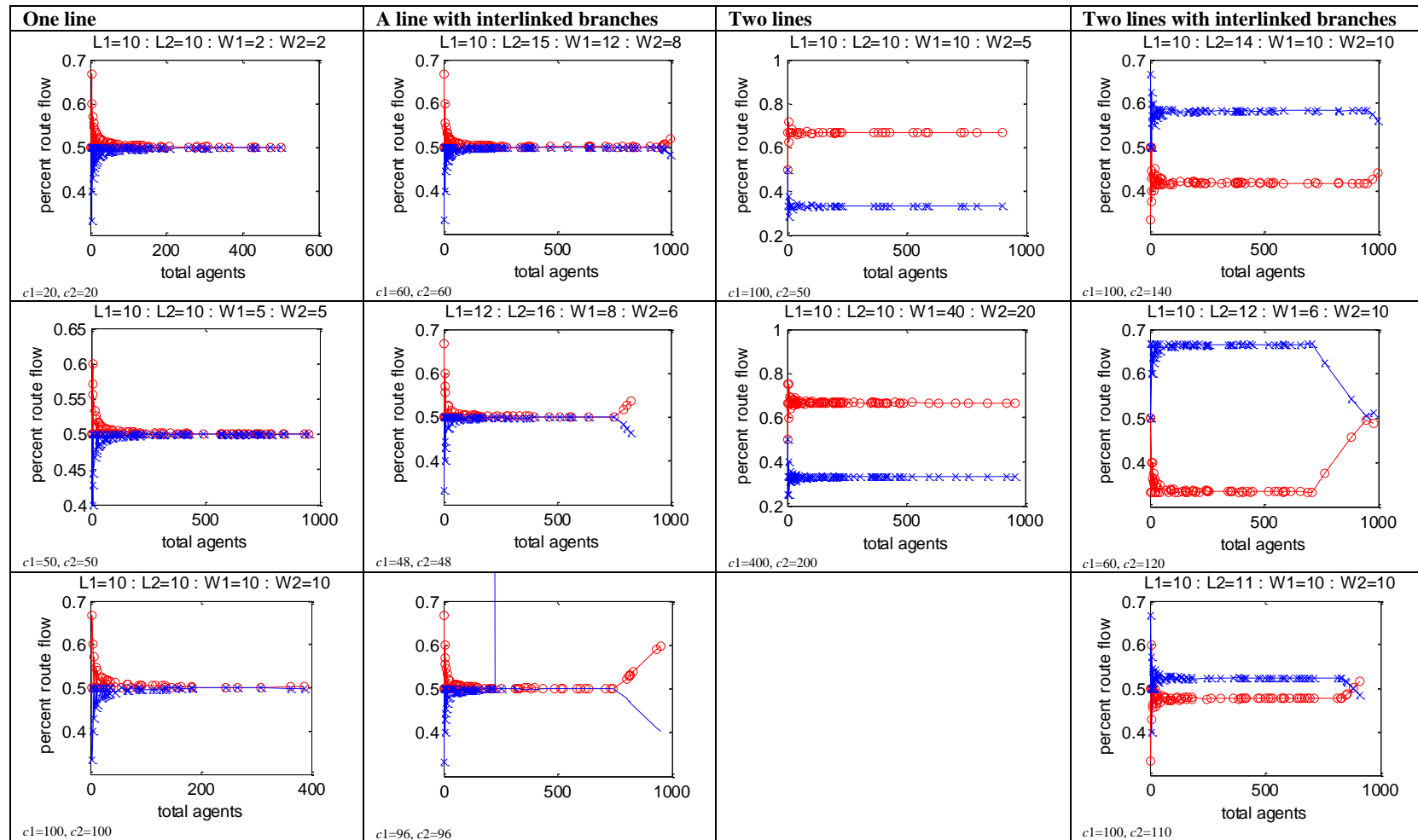
where  $L$  is the length,  $W$  is the width, and  $\rho_{\max}$  is the maximum density.

In our numerical experiments, we use meters for the length and widths of the edges. Our model also assumes that the maximum density is 4 persons per square meter. The computed threshold in each configuration agrees with that found in each of the plots. To account for the divergence in the plots we give the following explanation.

At the time when the threshold is reached, the 2 edges are completely filled up. The shorter edge, however, will start to release agents sooner than the other edge, thus becoming available again for accepting a few agents. Consequently, more agents pass through this edge than in the other. Until the longer edge starts to release agents, incoming agents will use the shorter one. This explains why the gap between the path usage ratios continues to increase immediately after the threshold point.

At some point, the change in path usage ratio for the 2 edges is inverted. That is, the edge that was previously experiencing an increase in the path usage ratio will start to experience a decrease because of congestion, while the other edge starts to have an increase in the ratio (as a result of the congestion on the other edge).

This next critical point actually corresponds to when the second edge starts to release some agents on the other end, and becomes available for incoming agents. These agents will therefore prefer this (unsaturated) edge over the other (saturated) one.



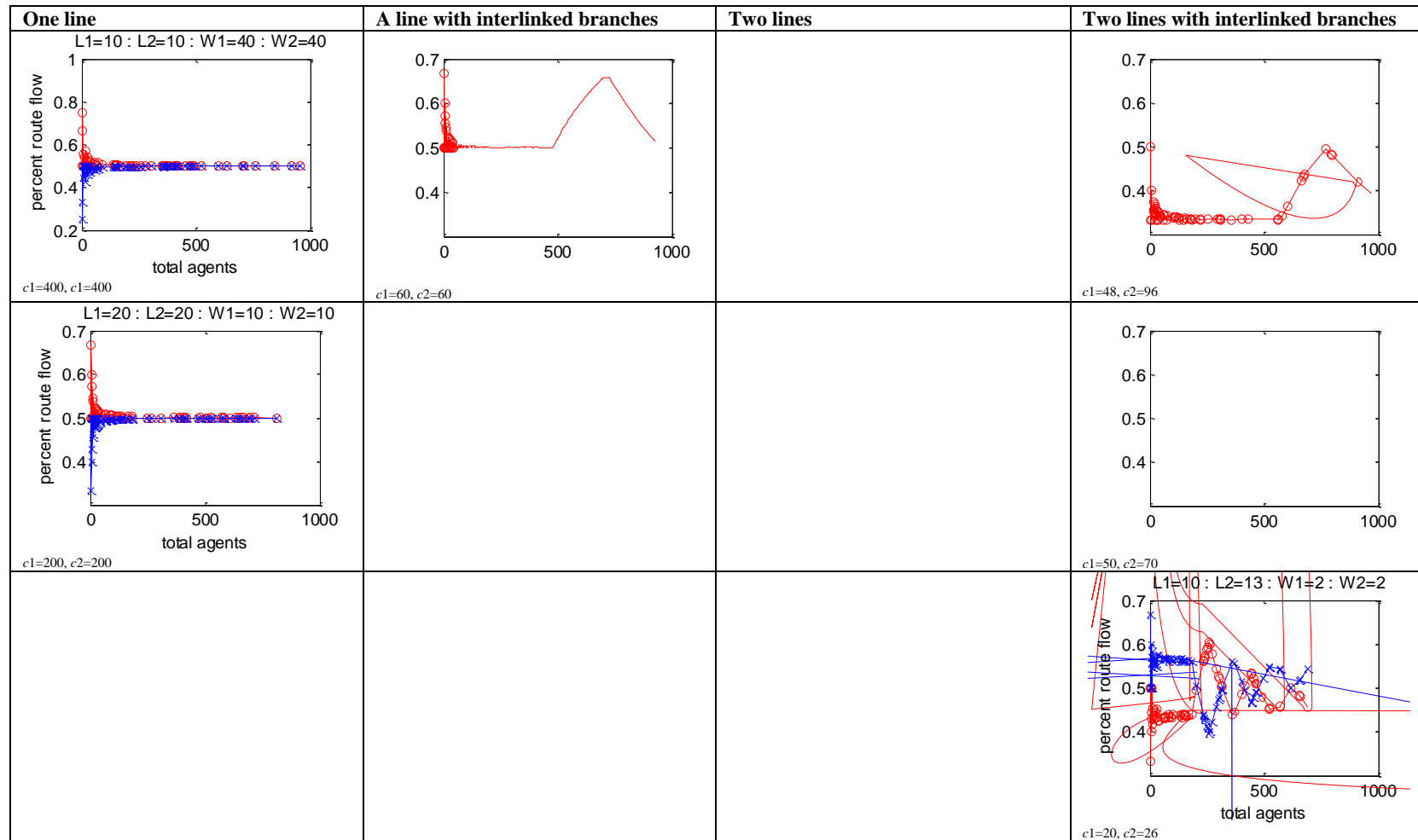


**Figure 6.** Four basic patterns observed from the plots of path usage ratios.

Numerically, this second critical point can be computed by deriving some pieces of information.

1. First, the time  $t_{out}$  it takes for the first agent in the longer edge to come out can be computed by  $t_{out} = L_2 / u_{init}$  where  $L_2$  is the length of the longer edge and  $u_{init}$  is the speed of the first agent that entered this edge.
2. Next, the time it takes for each of the first  $k$  agents in the shorter edge can be computed using a similar formula, i.e.,  $t_k = L_1 / u_k$ . Then we evaluate the maximum  $k$  such that  $t_k < t_{out}$ . This  $k$  value is the second critical point.

Two other important aspects of the second pattern should be emphasized:

1. For a single line to be observed on the left part of the plots, the 2 edges should have the same space capacity values. This ensures that both have equal attractiveness at the start. If the space capacities are not the same, then there will be 2 lines on the left part of the plot, as explained in the third pattern.
2. After initially filling up the 2 edges, incoming agents will have to wait for agents coming out of one of the edges. For each edge, there will be no simultaneous exit (i.e., only maximum one agent exits at a given time). Consequently, each future incoming agent sees exactly  $c - 1$  agents in the edge, where  $c$  is the space capacity. Thus every such agent will have the same initial speed. Considering this fact on agents of both edges, the increase-decrease pattern in path usage ratios is guaranteed to be rhythmical.

### *Pattern 3: Two Lines*

In the cases covered by this pattern, the plots are asymptotic to the 2 lines at ratios  $r_1$  and  $r_2$ . Such cases occur *only* when the lengths of the edges are equal, while the widths are unequal. The explanation for this observation is given as follows.

Let  $l_1$ ,  $l_2$ ,  $w_1$  and  $w_2$  be the lengths and the widths of the 2 edges, with  $l_1 = l_2$ , and, without loss of generality, let  $w_1 < w_2$ . If we let  $k = w_2/w_1$  be the ratio of the 2 widths, then it follows that the ratio of the space capacities of the 2 edges is also equal to  $k$ . That is,  $c_2/c_1 = k$ .

To simplify the discussion, assume first that  $k$  is an integer. At the beginning, both (empty) edges are equally attractive, in terms of their interaction value  $I_{e,t}$ . The first edge gets the first agent, making it less attractive after. Succeeding  $k$  agents will select the second edge, after which the interaction values for the two edges would have equalized again. In other words, for every agent that goes to the first edge,  $k$  succeeding agents choose the second edge. This leads to the following values for  $r_1$  and  $r_2$ .

$$r_1 = \frac{1}{k+1}, r_2 = \frac{k}{k+1} \quad (7)$$

Writing these in terms of the space capacities, then since  $c_2/c_1 = k$ , we have the following results.

$$r_1 = \frac{c_1}{c_1 + c_2}, r_2 = \frac{c_2}{c_1 + c_2} \quad (8)$$

In the case that  $k$  is not an integer, the plots are just not as straight (since ceiling values have to be accounted for) but are still asymptotic to the computed  $r_1$  and  $r_2$  values.

#### *Pattern 4: Two Lines with interlinked branches*

Cases for this type actually combine properties from the 2 previous cases. In particular, they cover the cases when the lengths are unequal (Pattern 2), and at the same time the space capacities are unequal (Pattern 3).

At the start of the simulation, the phenomenon observed in pattern 3 is also observed, i.e., that of having 2 separate lines at  $r_1$  and  $r_2$ ; - - - - - 9 - - - - -  
- - - - - ; - 9 - - - - -  $r_1$  and  $r_2$  use the same formula as in the previous case.

The presence of interlinked branches in the plots is also explained by the inequality in the lengths of the edges. The critical point at which the branching starts to occur is given at the point when the number of agents is  $n = c_1 + c_2$ , the sum of the space capacities of the 2 edges. As in the second case, the interlinking is periodic (sometimes covering several increase-decrease combinations). The reason for this is after the edges have been filled up, the succeeding agents that successfully enter a given edge will have exactly the same velocity as the last agent that entered the same edge.

In summary, the 4 patterns may be described in 4 quadrants, determined by the relationship between the lengths and also the space capacities between the 2 edges, as illustrated in the table below

Table 1. Four basic patterns summarized in quadrants.

	<b>Equal capacities</b>	<b>Unequal capacities</b>
<b>Equal lengths</b>	Pattern 1: One line	Pattern 3: Two lines
<b>Unequal lengths</b>	Pattern 2: One line with interlinked branches	Pattern 4: Two lines with interlinked branches

The summarized information clearly shows that the usage is not only dependent on the distance (which the shortest path configuration assumes as the only factor), but also on the space capacity. This is the main reason why, as will be shown later, the normal RSCO is better than the shortest path configuration.

It should be noted further that there are 4 different patterns for the simple network in this study because in each of the two factors (i.e., length and capacity), there are 2 possibilities: equality and inequality.

If we extend the network to one with 3 edges from the source to the sink, then there will be more scenarios for each of the factors. In particular, for the length, if  $L_1$ ,  $L_2$  and  $L_3$  are the measurements for the edges, then, without loss of generality, there are 4 possible conditions:

1.  $L_1 = L_2 = L_3$
2.  $L_1 = L_2 < L_3$
3.  $L_1 < L_2 = L_3$
4.  $L_1 < L_2 < L_3$

All other possible configurations would be equivalent to one of these. For example, the condition  $L_1 = L_2 > L_3$  is actually equivalent to the 3<sup>rd</sup> item in the above list since the labeling of the edges may be interchanged. The 4 possible cases imply that the number of path usage patterns is  $4^2 = 16$ .

Similarly, for 4 edges connecting 2 nodes (the source and the sink), the number of possible cases are  $2^3$ , as shown below, and therefore the number of possible patterns is  $(2^3)^2 = 64$ .

1.  $L_1 = L_2 = L_3 = L_4$
2.  $L_1 = L_2 = L_3 < L_4$
3.  $L_1 = L_2 < L_3 = L_4$
4.  $L_1 < L_2 = L_3 = L_4$
5.  $L_1 = L_2 < L_3 < L_4$
6.  $L_1 < L_2 < L_3 = L_4$
7.  $L_1 < L_2 = L_3 < L_4$
8.  $L_1 < L_2 < L_3 < L_4$

It can be generalized that for a network on 2 vertices with  $n$  edges connecting the source to the sink, there would be exactly  $(2^{n-1})^2$  possible patterns. This can be derived by fixing the order of the edges. Then there are  $n-1$  possible adjacent binary relations, each with 2 possibilities;  $>$ ,  $=$ ,  $<$ . There are  $2^{n-1}$  possible length configurations. Similarly, there are  $2^{n-1}$  possible capacity configurations. The number of possible patterns is therefore  $(2^{n-1})^2$ .

Determining the number of possible patterns further becomes a lot more complex when a path from a source to a sink involves more than 1 edge, and especially if different paths overlap (i.e., there is a common edge). In any case, what has been clearly established in this part of the study is that to achieve the minimum egress time for a given network, the distance should not be the only factor; the space capacity of each edge is also a very important consideration.

## 5.2 Egress Time Comparisons

Before the egress times of the 3 different configurations are analyzed, we first examine the average speeds of the agents in a specific edge. Figure 7 shows a revealing result.

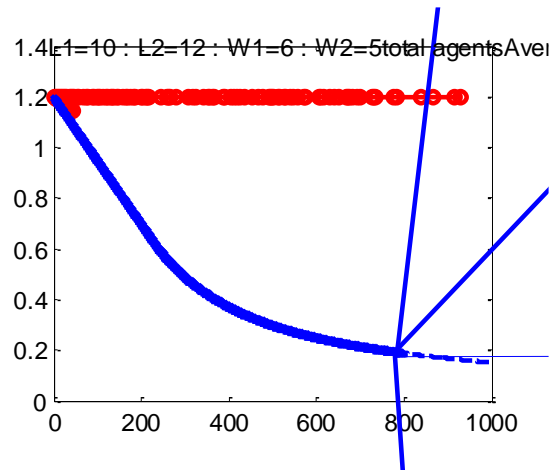


**Figure 7.** Comparing the average speed of the agents in the 3 configurations.

Observe that for the Minimum Egress RCSO, all the agents have the same speed, which is the maximum possible speed of 1.2 m/s. This will lead to the (theoretical) minimum egress time. However, this is also clearly not possible since it violates the flow-density relationship. The ordinary RCSO yields a more realistic flow-density diagram, and is further shown to be superior to the shortest path configuration.

Showing now the actual egress time, which is the main focus of this study, we see an interesting pattern as well (see Figure 8).

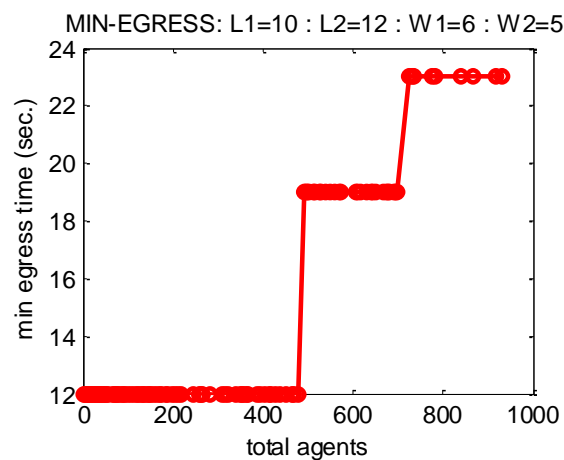


**Figure 8.** Total Agents vs. Egress Time for the Minimum Egress RCSO model.

There appears to be jumping levels, unlike the expected linear increase in egress time. Such behavior actually reflects the limitation of the model used, since an agent at a given discrete time step is only allowed to enter an edge if that - - - - - ; - - - - - speeds are not affected by the density (as inferred from Fig. 7), then if  $c$  is the space

capacity of the edge, exactly  $c$  agents are allowed to pass through that edge synchronously, from start to end.

Thus, the second level in the plot corresponds to the next batch of agents synchronously passing through that edge. If there are  $b$  batches of agents, then the plot will have exactly  $b$  level portions.

A revision of the algorithm can have the agents not simultaneously processed in a single discrete time-step. If lag time between agents is placed, then the plot would be more consistent with the theoretical egress time, as shown in Fig. 9.

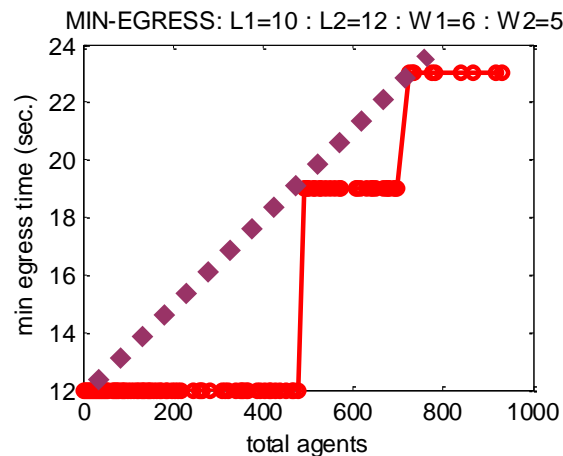


**Figure 9.** Minimum Egress RCSO vs. Theoretical Optimal Configuration.

Finally, we compare the results of the egress times from the 3 different models. The plot for this is shown in Fig. 10.

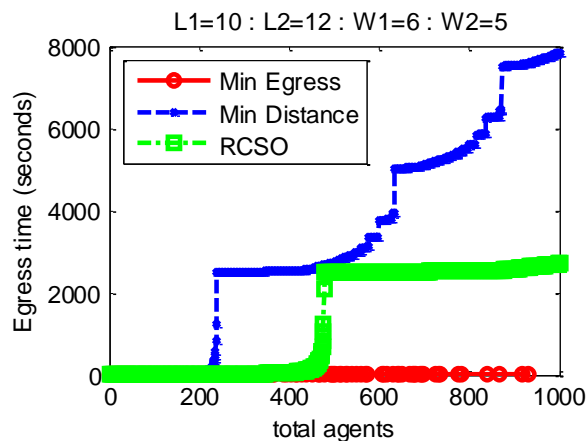


**Figure 10.** Egress times of the 3 models.

From the plot, it is clear that ordinary RCSO yields better egress time than the shortest path configuration. Although the egress time of the ordinary RCSO is bigger than that of the Minimum Egress RCSO, it still gives much improvement compared to the shortest path

configuration. In fact, the gap in the performance of ordinary RCSO compared with the shortest path generally increases with increasing crowd size.

An important implication of this last result is that when pedestrian facilities are not too crowded, then the shortest path configuration may yield good egress times (i.e., near the optimal solution). However, as the size of the crowd increases, such configuration leads to egress times that are too far from the theoretical optimal. Ordinary RCSO, in this case can approximate the theoretical optimal much better.

## 6. Conclusion

This study aims to simulate optimum egress time. By running SPSA with Tabu list to find the best parameter set for the (Minimum Egress) RCSO, a theoretical lower bound of the egress time was determined. For such configuration, it was observed that there are 4 emerging patterns on relative path usage. More importantly, the emerging relative path usage is a function mainly of 2 edge attributes: the length and space capacity. This gives us hints that the shortest path need not always be the preferred evacuation route because it fails to consider the other important edge attribute (space capacity).

Comparing the egress times of ordinary RCSO and shortest path configuration reveals that the ordinary RCSO approximates the minimum egress configuration better. RCSO relates to people adapting their behavior to local conditions whereas static evacuation maps provide a snapshot view of the routes/exits. One practical application of this result is to revise egress-helping items, such as evacuation maps, in order to encourage an evacuation that follows ordinary RCSO instead of the simple shortest path. For instance, instead of displaying only the shortest path in an evacuation map, a primary exit route and a secondary exit route may be displayed. Alternatively, the shortest path in some of the maps may be replaced by slightly longer (but more spacious) paths so that congestion on some paths may be decreased, leading to the emergence of an RCSO-like evacuation behavior.

When multiple routes are displayed on evacuation maps, the occupants can have options to alter their route choice. However, the exercise of such options by the occupants is not guaranteed. It is also not guaranteed that large crowds will follow the routes suggested on evacuation maps. It is not yet clear how influential the "following the crowd" - is against evacuation map information. Such possible deviations should be addressed in some further studies.

As a final note, the insights gathered in this study resulted from a simple network. It was shown that, as the number of edges increases, the number of possible path usage patterns increases exponentially. It would be very interesting to find some emerging patterns for these as well. Another direction, therefore, for further studies can investigate some major patterns for more complex networks.

## Acknowledgement

This research was funded by the Loyola Schools of the Ateneo de Manila University. The authors are grateful to the anonymous reviewers and Prof. Ed Galea for their useful comments and corrections.

## References

- Blue, V.J. and Adler, J.L., 2000. Cellular Automata Microsimulation of Bidirectional Pedestrian Flows, Transportation Research Board 1678, pp.135-141.
- Dafermos, Stella. C. and Sparrow, F.T., 1969. The Traffic Assignment Problem for a Traffic Network, *Mathematics of Operations Research*, 4(1), 91-118.
- Dial, R.. 1971, A probabilistic multipath traffic assignment model which obviates path enumeration, *Transportation Research*, 5 (2), 83-111.
- Florian, M., Mahut, M., and Tremblay, N., 2001. A Hybrid Optimization-Mesosopic Simulation Dynamic Traffic Assignment Model, *Proceedings of the 2001 IEEE Intelligent Transport Systems Conference*, 120-123.
- Greenshields, B.D., 1934, A study of traffic capacity, *Proc. Highway Research Board* 14: 448-477.
- Glover, F., 1989. "Tabu Search - Part I", *ORSA Journal on Computing* 1989 1: 3, 190-206.
- Helbing D. and Molnár P., 1995. Social force model for pedestrian dynamics, *Physical Review E* 51, 4282-4286.
- Henderson, L. F., 1974. On the Fluid Mechanic of Human Crowd Motions, *Transportation Research* 8, pp. 509-515.
- Hoogendoorn, S. P. and Bovy, P. H. L., 2004. Pedestrian route-choice and activity scheduling theory and models, *Transportation Research Part B: Methodological*, Volume 38, Issue 2, February 2004, 169-190.
- Kachroo, P. and Ozbay, K., 1999. *Feedback Control Theory for Dynamic Traffic Assignment*, Springer-Verlag, London.
- Lovas, G.G., 1994. Modeling and Simulation of Pedestrian Traffic Flow, *Transportation Research* 28B, 429-443.
- Schadschneider A., 2001. "Cellular automaton approach to pedestrian, dynamics-theory", in M. Schreckenberg, S. D. Sharma (eds.) *Pedestrian and Evacuation Dynamics*, Springer, Berlin

Schneider, V. and Könnecke, R., 2011. -- concepts and appl -- W. Klingsch, C. Roesch, A. Schadschneider, M. Schreckenberg (eds.) Pedestrian and Evacuation Dynamics 2008, Springer, Berlin

Spall, J.C., 1998. "An Overview of the Simultaneous Perturbation Method for Efficient Optimization," Johns Hopkins APL Technical Digest, vol. 19, pp. 482-492

Teknomo, K. and Millonig, A., 2007. A Navigation Algorithm for Pedestrian Simulation in Dynamic Environments, Proceeding of the 11th World Conference on Transport Research (WCTR), University of California, Berkeley, USA, June 24-28, 2007.

Teknomo, K., 2008. Modeling Mobile Traffic Agents On Network Simulation, Proceeding of the 16th Annual Conference of Transportation Science Society of the Philippines (TSSP), Metro Manila, Philippines, September 19, 2008.

Teknomo, K., Bauer, D. and Matyas, T., 2008. Pedestrian Route Choice Self-Organization, Proceeding of the 3rd international Symposium on Transport Simulations, Queensland, Australia August 6th-8th, 2008

Tolujew, J. and Alcalá, F., 2004. A Mesoscopic Approach to Modeling and Simulation of Pedestrian Traffic Flows, Proceedings 18th European Simulation Multiconference.

Tubbs, J.S. and Meacham, B.J., 2007, Egress Design Solutions -- A guide to evacuation and crowd management planning, ARUP.